

INCLUSION PRECIPITATION IN SUPERALLOYS

S.L. Cockcroft, T. Degawa*, A. Mitchell, D.W. Tripp, and A. Schmalz

Department of Metals and Materials Engineering
University of British Columbia
Vancouver BC, Canada
V6T 1Z4

*Presently with Advanced Materials and Products Division
Mitsui Engineering and Ship Building Co.
Tamano, Japan.

Abstract

Sufficient thermochemical data is now available to permit the computation of the precipitation conditions for TiN, MgO, MgS, and Al₂O₃ in a range of superalloy compositions. These computations have been carried out for a number of example cases, taking into account the segregation which takes place on freezing. The results have been used to illustrate the inclusion populations which might be expected when processing the alloys by various melting methods. The importance of composition and temperature in controlling the inclusion population is demonstrated in relation to the appropriate saturation solubilities. Using this data, optimum concentrations of O, N and S required to eliminate the problem of clustered inclusions have been suggested. The possibility of making alloys without any inclusions in the solid has also been assessed. It has been concluded that the composition requirements for "zero inclusion" wrought superalloys are within the capability of present commercial techniques. It has also been confirmed that the method of inclusion assessment by EB button melting is valid for oxide inclusions in superalloys, provided that it is carried out with sufficiently low superheat, but it is not a satisfactory method for collecting an assessing TiN inclusions.

Superalloys 1992
Edited by S.D. Antolovich, R.W. Stusrud, R.A. MacKay,
D.L. Anton, T. Khan, R.D. Kissinger, D.L. Klarstrom
The Minerals, Metals & Materials Society, 1992

Introduction

Most superalloy compositions contain sufficient reactive metal content that the solubility product of inclusions is extremely small. In consequence, at normal process temperatures, there is a dispersion of oxides and nitrides in equilibrium with the liquid metal together with the random occurrence of exogenous oxide inclusions, characteristic of metal processed in ceramic containers. The introduction into the industrial sequence of ceramic-less melting and casting has the potential to eliminate the exogenous inclusion problem. However, given the trend towards designing at the limit of the fracture properties of the material, the possible agglomeration of indigenous inclusions to give a defect of critical size becomes a significant problem. In alloys with a lower content of reactive elements (stainless steels and maraging steels), it has been demonstrated that nitrogen and oxygen levels can be achieved by electron beam melting which will not precipitate any inclusions at temperatures above the solidus since they do not exceed the solubility product of the relevant compounds even when accounting for the level of interdendritic segregation found in commercial ingots[1,2]. This "zero inclusion" technique can in principle be applied to superalloys, but their composition requirements will correspond to amounts of oxygen and nitrogen which are lower by a factor which depends on the reactive element content. It is the purpose of this study to suggest the limits of this composition requirement in relation to oxygen, sulphur and nitrogen in typical superalloys, given the processing conditions found in the remelting processes. In the context of these estimations, carbides are not considered to be inclusions since their solubility products are sufficiently high that they do not occur as solid particles in the alloys above the liquidus temperature.

Solubility Products

Thermochemical Considerations

The solubility product of titanium nitride in a superalloy may be defined as

$$K_S = [\text{wt}\% \text{Ti} \times f_{\text{Ti}}] \cdot [\text{wt}\% \text{N} \times f_{\text{N}}] \quad \dots(1)$$

for the reaction



where f_i is the Henrian activity coefficient of component i . For practical purposes, in this work, the product of the activity coefficients has been included in the solubility product constant, which is hence re-defined as

$$K_S' = [\text{wt}\% \text{Ti}][\text{wt}\% \text{N}] \quad \dots(3)$$

Equation (2) has a temperature dependence such that the equilibrium moves to the right with increasing temperature. It also has a composition dependence, controlled by the analytical content of Ti and N and by their activity coefficients. Apart from titanium and nitrogen, chromium has also been found[3] to exert a strong influence through the activity coefficient of nitrogen, a factor which has been noted frequently in a wide range of chromium-containing steels[4]-[6].



Solubility products for the oxides (more familiar as "deoxidation constants" in the steel industry) may be derived in the same manner and follow generally the same relation to temperature and composition in the various alloys as do the nitrides, with the exception that the Al - Al interaction is quite strong in this system and so the relationship shows the same inversion with increasing Al content as do the deoxidation relationships in steels. Using the data of Samuels-son[7], the saturation solubility of alumina in IN718 can be calculated on the basis of Equation (4), as shown in Figure 1. The saturation at the liquidus temperature of IN718 is not negligible in comparison to the oxygen content found in commercial alloys (5 - 10 ppm O), and so we would anticipate that some of this content would be in solution at the point where freezing begins. For example, at 1340°C, an alloy with 5 ppm total oxygen content would have 2.8 ppm present as precipitated alumina and 2.2 ppm as oxygen in solution assuming that the oxide/alloy system had attained chemical equilibrium. The value computed for the precipitated oxide content is remarkably close to that found for this alloy when measured by the electron-beam button melting technique (e.g. reference 8, Table IV). The most interesting feature of this examination, observed in Figure 1, is that the solubility of alumina will increase as aluminium segregation takes place during freezing and cooling, since the self-interaction parameter of aluminium overrides the effect

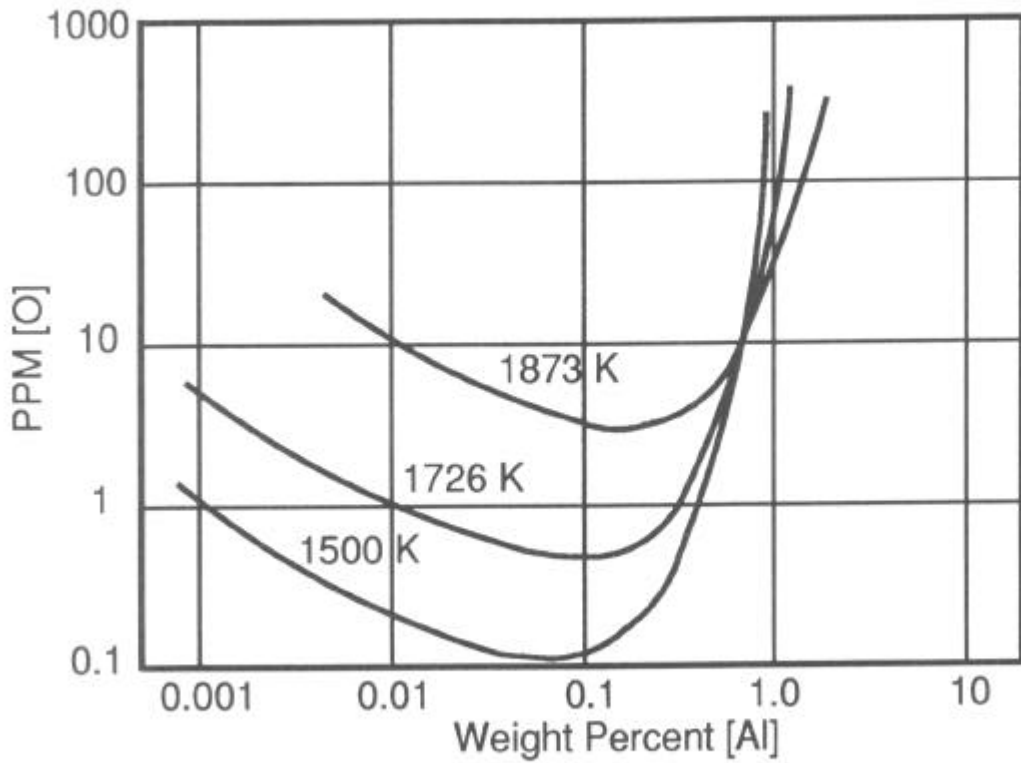


Figure 1 - Solubility product of alumina in IN718, using the data of Samuelsson[7].

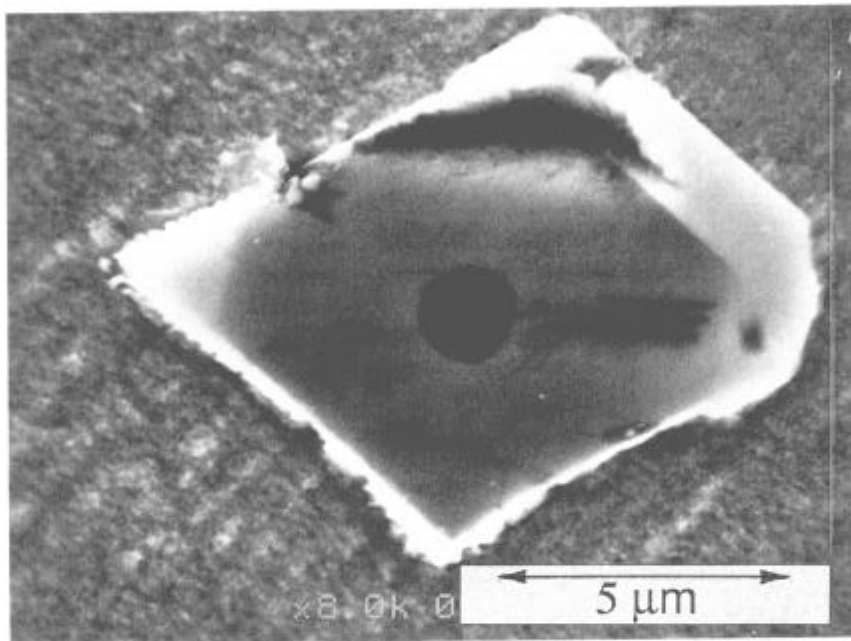


Figure 2 - Precipitation structure of a "carbo-nitride" in IN718, showing an $\text{MgO-Al}_2\text{O}_3$ core (note the hexagonal faceting) surrounded by TiN, which acted as the nucleant for a primary MC carbide (lighter-coloured coating on the TiN crystal).

of temperature on the solubility. The system will therefore not precipitate alumina in the liquid/solid zone. This is confirmed by the observation from experiment that neither carbides nor nitrides, which have precipitated in this region, contain alumina as the nucleating core.

In most wrought superalloys, the content of Mg is sufficiently high that it also forms oxide precipitates, as confirmed by a number of observations including; MgO cores in both oxide and nitride inclusions, and both isolated MgO and MgO·Al₂O₃ particles in the commercial alloy[8]. The solubility product of MgO is extremely small and the situation is further confused by the possibility of the precipitation of MgS inclusions. Computation of the MgS solubility product in a typical alloy composition using the data of Samuelsson[7], indicates that precipitation can take place only during solidification for the ranges of Mg and S found commercially. The observation of inclusions is hence complicated by segregation on freezing.

Based on thermodynamics[7] alone, MgO should be present as an equilibrium phase mainly in the form of MgO·Al₂O₃ at processing temperatures. It is highly likely, therefore, that the observed MgO particles are formed at very high local Mg concentrations during alloy addition (or are already present as MgO in the master alloy) and have not subsequently redissolved. Overall, at Mg contents in the range of 20 - 30 ppm, a very small proportion of the Mg will be present as precipitated oxide at the liquidus temperature leaving most of it available for other reactions as solidification proceeds. Since the Mg-O-MgO system has the same characteristics as the Al-O-Al₂O₃ system, it might be expected that no MgO would precipitate during freezing. However, since the activity of Mg in the alloys is much lower than that of Al, the opposite behaviour arises with cooling and segregation, in that, MgO would become more stable as solidification proceeds. An elementary mass balance, however, shows that this effect would be submerged by the much higher concentrations of aluminium present and we would not expect to observe any significant further precipitation of MgO during freezing. This is supported by the fact that smaller particles of TiN, precipitated close to the eutectic temperature, do not have cores of oxide particles of either MgO or alumina.

Effects of Segregation on TiN Precipitation

A notable characteristic of the superalloys is the extent to which they segregate on freezing. The solidification sequence is invariably complex[9] and the elements which are involved in inclusion precipitation reactions can be present at concentrations greatly enhanced over the bulk concentration. Hence, it is necessary to take into account not only the intrinsic temperature dependence of the solubility product but also the change in element concentration in the interdendritic liquid when estimating the extent of precipitation. This effect leads to a distinct duality in the inclusion population; those which have been precipitated on cooling in the liquid from the bulk composition, and those which have precipitated interdendritically as a result of segregation and cooling. The effect may be seen most clearly in the case of IN718 and its population of TiN inclusions[3]. The solubility of N in IN718 at 1700K, as determined from the solubility product of TiN, is approximately 38ppm N, which implies that in the typical wrought commercial alloy at 60 ppm N, approximately 1/3 of the total N content will be present at that temperature as solid TiN particles in the liquid. The implications of this finding in relation to the efficacy of filtering techniques has been previously discussed[10]. Experimental work indicates that most of the remainder is precipitated between the liquidus and solidus, with approximately 1 ppm N in solution at the end of freezing and available for precipitation in the solid state. Whilst the precipitation during freezing will not result in the large agglomerations of inclusions constituting critical flaws in the alloy[3], it probably has a significant influence on the nucleation and growth of primary MC carbides, and hence on their size distribution, since the fraction of the latter which nucleate above the final eutectic temperature invariably grow with a TiN core as shown in Figure 2.

The precipitation arising from segregation is given by combining the relationships governing the temperature dependence of the solubility product and the temperature dependence of composition. The latter is simply described by the Scheil equation [11]

$$C_L = C_0(1 - f_s)^{k_0 - 1} \quad \dots(5)$$

provided the relation between the fraction solidified and temperature during freezing and the segregation behaviour of the constituent elements are known. The precipitation effect in relation to solidification segregation has been analyzed in detail for alumina in stainless steels and Maraging steels[1,2].

Figure 3 shows the results of this calculation in IN718 and demonstrates that at the point of initiation of primary carbide precipitation (1280 to 1290°C), the titanium concentration has risen to 4 wt%. Assuming that no additional correction is necessary for nitrogen segregation, it is clear that the combination of temperature and segregation makes TiN very insoluble, reducing the solution nitrogen to the range of 1 - 2 ppm N. The equilibrium saturated solution at the liquidus point would therefore precipitate almost all of its nitrogen content before the carbide precipitation takes place. This is demonstrated by the fact that the large primary carbides have a nucleating core of TiN. It is important to realize, that not all of the TiN particles have a carbide envelope since they can be incorporated in the growth of the gamma dendrite before the temperature has fallen to the point of nucleating carbides.

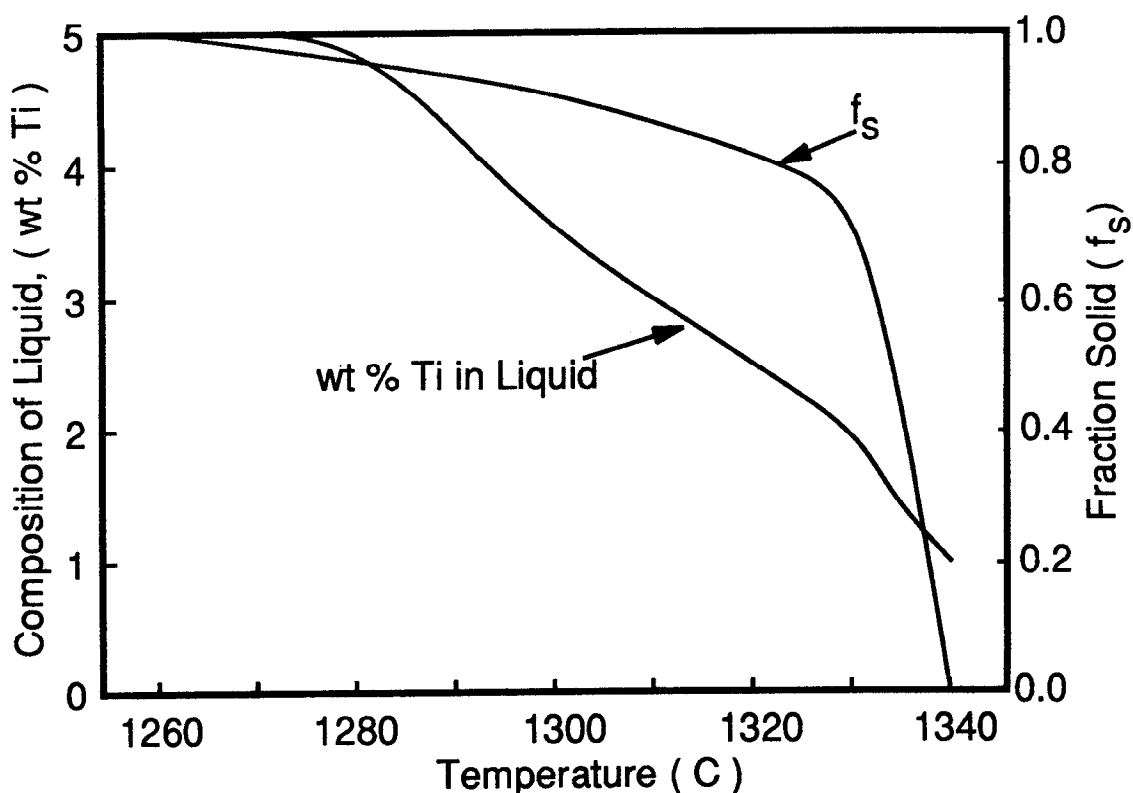
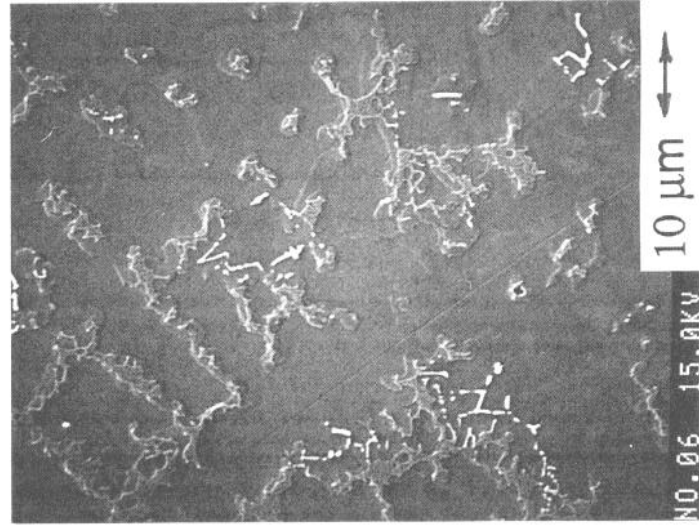


Figure 3 - Temperature dependence of interdentritic segregation of titanium and fraction solidified in IN718.

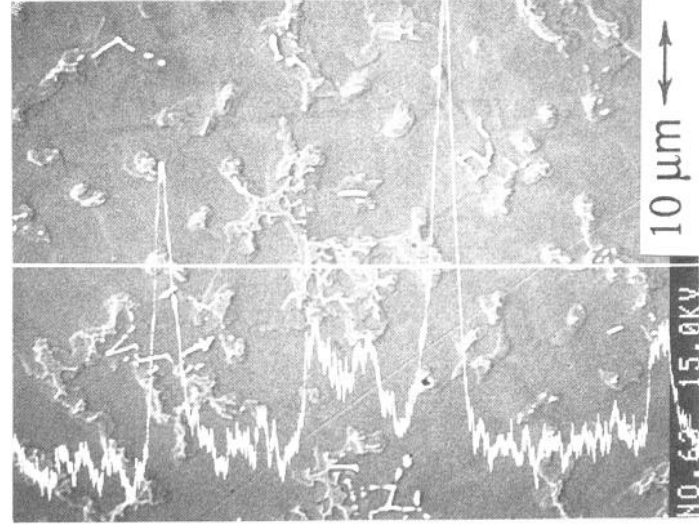
Segregation Effects on MgS Precipitation.

The precipitation of MgS presents an interesting case in commercial superalloy compositions, since, as indicated previously Mg and S, are at concentrations which clearly represent a complete solution at the temperatures normally found in the liquid during remelting processes. Therefore, inclusions of MgS in the solid would expect to be found only during freezing in the interdendritic structure and never in dendrite core regions or in samples quenched from the liquid.

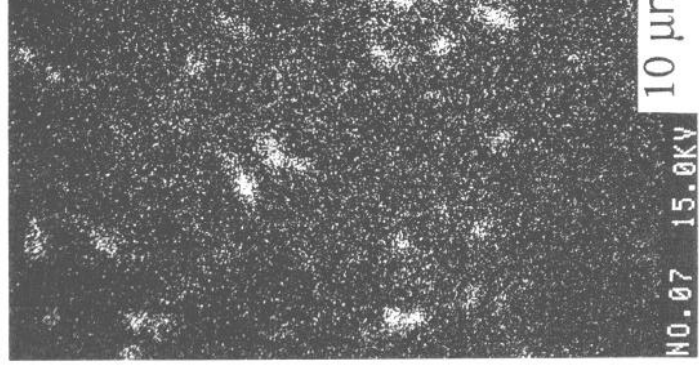
To verify this, a series of IN718 samples, with compositions shown in Table I, were prepared by laboratory vacuum induction melting followed by directional solidification, under the thermal conditions computed to exist at the centreline of a 500mm dia VAR ingot made under typical commercial operating conditions (Local Solidification Time = 800 sec.). The experimental conditions and VAR model have been described previously[12]. The samples were examined by both optical and electron optics techniques (SEM/EPMA) after surface preparation using non-aqueous media and additional precautions to prevent the hydrolytic decomposition of either MgS or CaS inclusions. An example of the structure found for sample T60 is shown in Figure 4. No CaS or other sulphide compositions were observed. The photomicrographs reveal that the sulphide inclusions are clearly in the last volume to be precipitated on freezing and that none of the inclusions were found in an intra-dendritic position. With regard to the effect of composition, examination



(a)



(b)



(c)

Figure 4 - SEM Examination of Sample T60 (Table 1), x 1000: (a) BSE image; (b) linear analysis for sulphur; (c) X-ray map for sulphur.

of sample T270 revealed only the occasional MgS precipitate, whereas in sample T420, they were absence. Since the freezing (and hence the segregation) conditions examined were the "worst-case" representing the centreline of a commercial ingot the following criterion for the presence of MgS primary precipitates in IN718 can be established: *for an Mg content of 30 ppm; S must be less than 25 ppm.*

Table I
Sample Chemistry

Sample #	S (ppm)	Mg (ppm)	Ca (ppm)	N (ppm)
Blank	<1	30	20	14
T60	107	30	10	14
T210	54	30	<10	12
T240	41	30	<10	12
T270	27	30	20	13
T420	9	40	10	14

Implications for Superalloy Processing.

The present goal of conventional superalloy melting processes is to produce an alloy which has no content of exogenous inclusions. This objective addresses the concerns of the user in regard to the predictability of fracture and fatigue behaviour, summarized by studies such as those by Pineau[13]. The basic problem faced by the user and producer alike is that of assessing from routine analysis when this situation has in fact been attained. The correlation between properties and bulk chemical composition is, as expected, quite poor at low impurity contents and is found to be process dependent. It is important, therefore, that the role of the process in inclusion removal be understood.

Table II
Saturation Solubility of TiN in IN718

T (K)	P_{N_2} (atm)	Saturation [N] (ppm)
1700	4.8×10^{-5}	39
1800	4.0×10^{-4}	112
1900	2.7×10^{-3}	290
2000	1.2×10^{-2}	620

Removal of TiN - The saturation solubility relationships for titanium nitride as a function of temperature, lead to the values for P_{N_2} and [N] presented in Table II. It is clear from this data, that if the alloy is processed at an elevated temperature, nitrogen will go into solution and subsequently be re-precipitated at a lower temperature during cooling and solidification. Regardless of the chosen route for removal of TiN, it is essential to use the minimum temperature possible. One possible advantage of electron beam is that the temperature of the molten pool as a whole may be kept low while the incident temperature under the beam target is extremely high. Since the vacuum decomposition of TiN floating on the surface will be much faster than its decomposition

by diffusion into the liquid, it is likely that TiN particles intercepted by the direct beam will be volatilized to contribute to the overall loss of TiN by the various possible physical removal mechanisms.

The TiN inclusion content in the liquid alloy will become zero when the nitrogen content is less than the saturation solubility of TiN - e.g. 38 ppm N in the case of IN718 at 1700K. A threshold value for nitrogen might be established, but it is not yet clear how this value should be defined, since several other factors must be taken into account. Given the rather coarse dendritic nature of solidification in superalloy ingots and the evident extent of interdendritic flow, it may not be possible to eliminate inclusion agglomeration merely by eliminating TiN particles at the liquidus temperature, since they will continue to form in the interdendritic region and could possibly agglomerate in the liquid flows of that region. Owing to the lower density of TiN relative to that of liquid IN718, buoyancy forces may also play a role in agglomeration allowing TiN inclusions to escape the solidifying matrix. However, no evidence has yet been found to either support or disprove this hypothesis.

From a processing standpoint, once all of the TiN has been removed from the liquid, a different regime of nitrogen removal is entered - desorption of N₂ from the free metal surface. This has been shown by numerous workers to be a very slow process, even in alloys with a low oxygen potential[14]. In addition, the partial pressure requirements are also severe. As can be seen from the data presented in Table III, in order to fulfill the requirements of the absence of TiN during freezing the alloy would have to be processed at a temperature close to the liquidus under a vacuum of better than 1 micron partial pressure of nitrogen (a higher process temperature would require a correspondingly lower nitrogen partial pressure to achieve the same result). This range of pressure is lower than that commonly found in melting for wrought applications, but is well within the design capability of conventional vacuum systems for both VIM and EB. It is interesting to note that the values given in Table III correspond very well to the limiting values found in small scale experiments[15] in which high-purity argon gas was bubbled through IN718 at 1450°C in a 5Kg VIM furnace at an ambient pressure of 10⁻⁵ atm. The concentration found was 7 - 8 ppm N, and although the actual nitrogen partial pressure in the argon gas was not given, a typical value for a highly-purified laboratory gas would be 1ppm N₂, or approximately 1 x 10⁻⁶ atm, in agreement with that calculated.

Table III
Relationship Between Nitrogen Partial Pressure
and
Nitrogen Solution Concentration in IN718 at 1700K

P_{N_2} (atm)	[N] (ppm)
4.8×10^{-5}	39
1.9×10^{-5}	25
3.2×10^{-6}	10
7.9×10^{-7}	5

Perhaps a more pragmatic approach to melt processing would be to restrict the nitrogen content to one which will prevent TiN precipitation until quite late in the solidification scheme - for example, until the point of primary carbide nucleation. Following the derivations of the segregation scheme outlined above, this level would be in the region of 1 - 2 ppm, which implies that we could retain the nucleating effect of the nitride but avoid any agglomeration if the nitrogen content is lower than 4 - 5 ppm, giving the first appearance of nitrides at a temperature slightly above that of the primary carbide nucleation point.

The temperature gradients observed in the VAR melting of IN718 are also of interest in the nitride process path. Values computed for typical melting conditions indicate that the maximum temperatures in the process are approximately 1700K. In the best condition of metal being fed from the electrode into the pool, the process can be expected to have the potential for removing TiN inclusions down to the saturation solubility at 1700K - i.e. 39 ppm N. The solid inclusions would be swept to the ingot periphery by metal flow and become trapped at that point (accounting for the elevated levels of nitrogen found in the ingot surfaces of both VAR and ESR ingots). This mechanism, however, would not eliminate the possibility of TiN agglomerations in the ingot since the same metal flows could also sweep the TiN collections into the body of the ingot. The ambient vacuum in the VAR furnace does not provide a low enough partial pressure of nitrogen to reduce the content significantly below 39 ppm N at 1700K, and so, even if the kinetics of de-nitrogenization would permit the reaction to go to completion the ingot would still not be in the desired range of composition.

Removal of Oxides - From the analysis present earlier, it is evident that almost all of the analytical oxygen content is contained in either exogenous inclusions or in precipitated alumina inclusions in the liquid. If an oxygen content less than this latter value is achieved at the liquidus temperature, then no further oxide inclusions will precipitate during freezing. Thus, in a relatively straight forward manner, it is possible to establish a threshold value for oxygen content, below which oxide inclusions will not be present in the product.

Inclusions Assessment - The method of inclusion assessment by electron-beam button melting can be examined in the same way. The temperature profiles in an 8 cm diameter EB button, being heated with a 10 kW beam, following a 6 cm diameter circular path, were calculated using an FEM model and the results revealed that the centre portion of the button has only a thin liquid layer and so would collect TiN inclusions falling into this region in a quantity corresponding to the saturation solubility at the liquidus - i.e. approximately 25ppm N. Any TiN particles encountering the higher temperatures would dissolve, and given the duration of the test, it is unlikely that particles precipitated on cooling would float to the surface in the time available. In contrast, if the test is carried out incorrectly, with the beam following a circular path of 3 cm diameter, then based on the predicted temperature profiles probably no TiN collection would take place since it would all dissolve. Therefore, for a successful test it is necessary to programme the electron beam carefully (as has been noted in many practical descriptions of the method). For the case of assessing the oxide inclusion content, the arguments presented earlier conclude that no further precipitation of oxide inclusions will occur during freezing, and therefore, the EB button test will reveal all of the oxides present in the original alloy. It should also be noted that the inclusions collected are not floated from the body of the melt, but rather are those which were rejected by surface tension and remain on the surface until they are pushed to the centre in the last material to solidify.

In addition to beam path, the ambient vacuum conditions in the normal EB button test are of importance since a balance must be achieved between avoiding contamination by oxygen, at the very low levels of oxide inclusions encountered, and avoiding decomposition of the nitride inclusions. The best solution to this dilemma is probably to ensure that the system is extremely leak-tight and operate at pressure levels not below 10 microns in the melting chamber.

Table IV
Zero Inclusion Composition in ppm for IN718

S	Mg	N	O
2	5	5	2

The "Zero Inclusion" Goal - Based on the above data, it is possible to define the conditions for the "zero inclusion" objective. It will be necessary to process the alloy so that all exogenous inclusions have been removed; by for example, EB hearth melting; by adjusting the sulphur and magnesium contents to a level less than the solid solubility of MgS; and, by lowering the nitrogen content to a value which is equal to the solubility product of TiN at the precipitation temperature

of the primary carbides. Under these conditions, the solid alloy will contain no particles which are not assessable by random sampling and optical metallography. The mechanical properties of the alloy would therefore meet the desired design target of uniform and predictable behaviour in service. In the example case of IN718, the composition limits, presented in Table IV, appear reasonably achievable. For alloys with different contents of Al and Ti the values will be changed to maintain the appropriate relationships to the solubility products, but within the normal range of gamma-prime alloys the resulting compositions are within the expectations of modern processing.

Conclusions

An examination of the solubility relationships of inclusion-forming material in the gamma-prime superalloys shows that the "zero inclusion" goal can be attained with processing techniques available to the industry at present. Such processing will need scrupulous attention to the chemical thermal requirements of the technique, but does not require any in-principle development of new technology. It is to be anticipated that the alloys made following these rules will permit the designer a very considerable extra advantage in application. It has also been concluded that the electron-beam button test method for the assessment of oxide inclusions is valid if the button can be formed with negligible superheat, but it is not a satisfactory way to collect and assess nitride inclusions.

Acknowledgements

The authors gratefully acknowledge the support of the Nickel Development Institute and the Natural Science and Engineering Council of Canada during the course of this work.

References

1. A. Mitchell and S. Fukumoto, Proc. Vac. Metallurgy Conf., Pittsburgh Sept. 1991 (publ. Iron & Steel Soc. of AIME, Warrendale PA), in press.
2. A. Mitchell and S. Fukumoto, Proc. "Clean Steel IV" Conference, Balatonfured, Hungary, June 1992 (publ. institute of Metals, London, UK) in press.
3. A. Mitchell, "Advanced Materials and Processing Techniques", (publ. ASM Europe, Paris 1987), 233 - 241.
4. L. Liao and J.Fruehan, Trans. Iron & Steel Soc. AIME, 1989, Oct., 91 - 97.
5. H. Wada and R.D Pehlke, Met. Trans., 1977, 8B, 675 - 682.
6. D.S.Shahapurkar and W.M.Small, Met. Trans., 1987, 18B, 231 - 235.
7. E. Samuelsson and A. Mitchell, Met. Trans., in press.
8. W.H.Sutton, Proc. 8th International Conference on Vacuum Metallurgy, (Japanese Iron & Steel Institute, Tokyo, 1982), 2, 1420 - 1428.
9. G.K. Bouse, Superalloy 718 - Metallurgy and Applications, ed. E.A. Loria, (The Minerals, Metals & Materials Society 1989), 74.
10. A. Mitchell, International Iron & Steel Journal of Japan, 1992, May, in press.
11. M.C.Flemings, "Solidification Processing", (publ. McGraw-Hill, New York USA, 1974).
12. A. S. Ballantyne, J.F. Wadier and A. Mitchell, Proc. 6th International Conference on Vacuum Metallurgy, eds. G.K.Bhat and R. Schlatter (AVS, New York USA) 1976, 599 - 624.
13. A. Pineau; "High Temperature Materials for Power Engineering", eds E. Bachelet et al., (Kluwer Academic Publishers, Boston, USA), 1990, II, 913 - 934.
14. V.G.Volkov, E.V.Zameshaev, A.G.Totok and V.S.Dub, *ibid.* 150 - 159.
15. Xie X., Chen C., Shi W., Pu H., Jin J., Proc. 10th International Vacuum Metallurgy Conference, eds. Fu J., Zhang R., Xie X. and Bloore E. (publ. Metallurgical Industry Press, Beijing, China), 1990, 114 - 121.